Nonlinear Stabilization of a 3 Degrees-of-Freedom Magnetic Levitation System

Rafael Becerril-Arreola and Manfredi Maggiore[1]
Department of Electrical and Computer Engineering
University of Toronto, Toronto ON, Canada, M5S 3G4

Abstract

We consider the problem of controlling the position of a platen levitated using linear motors in the three-dimensional space. This theoretical study relies on a model developed in [3] and provides two controllers that solve the set-point stabilization problem. The first controller is derived by decomposing the model in two subsystems, applying feedback linearization to one of them, and using the invariance principle to prove attractiveness of the origin of the second subsystem. The second controller is found by feedback linearizing the entire system dynamics and using a recent result on invariance control to guarantee that the state of the system does not exit the set where the feedback linearizing transformation is well-defined.

1 Introduction

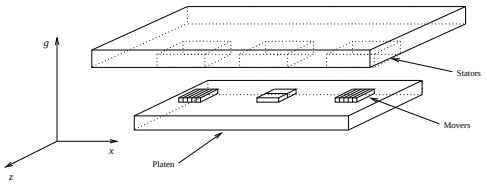

Figure 1: Configuration with three LSMs to achieve three degrees of freedom

In order to use linear motors in ultra-clean environments, the use of bearings and mechanical transmissions must be avoided. Bearings can be replaced by magnetic levitation, which has been already successfully implemented in [1]. In this paper, we present a different solution which deploys commercial technology and presents a challenging control problem. Our control design is based on the model developed in [3], which describes the setup shown in Figure 1, where three PMLSMs (Permanent Magnet Linear Synchronous Motors) are used to control the position of the platen. The model is given by

$$\begin{aligned}
\dot{x}_1 &= x_2 \\
\dot{x}_2 &= G - \phi(x_1)[2u_1^2 + u_2^2 + 2u_3^2 + u_4^2] \\
&\qquad - \tilde{\chi}(x_1) - \psi(x_1)[2u_3 + u_4] \\
\dot{x}_3 &= x_4 \\
\dot{x}_4 &= \gamma(x_1)u_2 \\
\dot{x}_5 &= x_6 \\
\dot{x}_6 &= 2\gamma(x_1)u_1,
\end{aligned} \tag{1}$$

where

$$\begin{aligned}
\phi(x_1) &= \beth \frac{\Gamma(x_1)\coth^2\left[\frac{\pi}{\tau}(x_1+h_m)\right]}{K_c^2(x_1)} \\
\psi(x_1) &= \frac{\nu\Gamma(x_1)B_{pmy}(x_1)\coth\left[\frac{\pi}{\tau}(x_1+h_m)\right]}{K_c(x_1)} \\
\gamma(x_1) &= \frac{\gimel\left[\eta - \frac{\zeta}{x_1+\kappa}\right]}{K_c(x_1)\sinh\left[\frac{\pi}{\tau}(x_1+h_m)\right]} \\
\tilde{\chi}(x_1) &= \chi\Gamma(x_1)B_{pmy}^2(x_1)
\end{aligned} \tag{2}$$

$\Gamma(\cdot)$, $B_{pmy}(\cdot)$ and $K_c(\cdot)$ are smooth nonlinear functions, ν, $\gimel$, h_m, $\beth$, χ and κ are known constants, and $u_1 \dots u_4$ are the control inputs.

The state is $\mathbf{x} = [x_1, x_2, x_3, x_4, x_5, x_6]^T = [g, \dot{g}, x, \dot{x}, z, \dot{z}]^T$, where g is the motors' airgap length and x and z are the platen's displacements in the x and y directions. Table 1 lists the values of the constants used in simulation.

Table 1: Simulation parameters for the 3DOF system

$\beth$	130.0188	χ	124,500
ν	4645.7	$\gimel$	19.5617
κ	0.0079	η	0.7071
ζ	0.0017	h_m	0.002

The functions $\tilde{\chi}(r)$ and $\phi(r)$ share the same sign, which is determined by $\Gamma(r)$. $\psi(r)$ has the same sign as $\phi(r)$ for $r > -h_m$. Due to both these properties and the squared inputs, stabilizing controls exist only for a range of values of x_1 - consider the problem of making $\dot{x}_2 = 0$ when u_1 and u_2 are given.

[1]This work was supported by the Natural Sciences and Engineering Research Council of Canada (NSERC)

We investigate the set-point stabilization problem for system (1) through two nonlinear approaches. The first approach, presented in Section 2, is based on partial feedback linearization and Lyapunov theory. In Section 3, full feedback linearization and invariance control are applied. Each section presents simulation results. Finally, after a comparison of the performance of both controllers, Section 5 presents a brief discussion.

2 Lyapunov Control

System (1) is composed of three subsystems, two of which are feedback linearizable. Let $\mathbf{x}^d = [x_1^d, \ldots, x_6^d]^T$ be the coordinates of the desired equilibrium point. Define $\tilde{\mathbf{x}} = \mathbf{x} - \mathbf{x}^d$.

Theorem 1 *The controller*

$$\begin{aligned} u_1 &= \frac{v_2}{2\gamma(x_1)} \\ u_2 &= \frac{v_1}{\gamma(x_1)} \\ u_3 &= 0 \\ u_4 &= -\frac{\psi(x_1) \pm \sqrt{\psi(x_1)^2 + 4\phi(x_1)R(\tilde{\mathbf{x}}^1)}}{2\phi(x_1)} \\ R(\tilde{\mathbf{x}}) &= \tilde{\epsilon}\left(\tilde{x}_1 + \tilde{x}_2\right)\left[\tilde{x}_1^2 + \tilde{x}_2^2\right] + \tilde{x}_2 \\ &\quad - \phi(x_1)U(\tilde{\mathbf{x}}) + G - \tilde{\chi}(x_1) \\ U(\tilde{\mathbf{x}}) &= 2\left(\frac{v_2(\tilde{\mathbf{x}}^2)}{2\gamma(\tilde{x}_1 + x_1^d)}\right)^2 + \left(\frac{v_1(\tilde{\mathbf{x}}^2)}{\gamma(\tilde{x}_1 + x_1^d)}\right)^2 \\ \begin{bmatrix} v_1 \\ v_2 \end{bmatrix} &= -K\tilde{\mathbf{x}}^2 \end{aligned} \tag{3}$$

makes $\mathbf{x}^d$ an attractive equilibrium point of (1), and the set $\mathcal{V}_d \times \mathcal{W} = \left\{\tilde{\mathbf{x}}^1 \in \mathbb{R}^2 \middle| \frac{\tilde{x}_1^2}{2} + \frac{(\tilde{x}_1+\tilde{x}_2)^2}{2} \leq d\right\} \times \left\{\tilde{\mathbf{x}}^2 \in \mathbb{R}^4 | \omega_1 \geq |\tilde{x}_i|,\ i = 3, \ldots, 6\right\}$ is contained in its domain of attraction, where the values of d and ω_i depend on the set-point $\mathbf{x}^d$ and are specified in the proof.

Proof. The closed-loop system reads as

$$\tilde{\mathbf{x}}^1 \quad : \quad \begin{cases} \dot{\tilde{x}}_1 = \tilde{x}_2 \\ \dot{\tilde{x}}_2 = -\tilde{\epsilon}\left(\tilde{x}_1 + \tilde{x}_2\right)\left[\tilde{x}_1^2 + \tilde{x}_2^2\right] - \tilde{x}_2 \end{cases} \tag{4}$$

$$\tilde{\mathbf{x}}^2 \quad : \quad \begin{cases} \dot{\tilde{x}}_3 = \tilde{x}_4 \\ \dot{\tilde{x}}_4 = v_1 \\ \dot{\tilde{x}}_5 = \tilde{x}_6 \\ \dot{\tilde{x}}_6 = v_2 \end{cases} \tag{5}$$

where $\tilde{\mathbf{x}}^1 := [\tilde{x}_1, \tilde{x}_2]^T$, $\tilde{\mathbf{x}}^2 := [\tilde{x}_3, \ldots, \tilde{x}_6]^T$, and the parameter $\tilde{\epsilon}$ adjusts the speed of convergence of the nonlinear dynamics.

The system $\tilde{\mathbf{x}}^2$ is written in matrix form as

$$\dot{\tilde{x}}^2 = A_c\tilde{\mathbf{x}}^2 + B_c\mathbf{v} \tag{6}$$

where $\mathbf{v} = [v_1, v_2]^T$ and (A_c, B_c) is controllable. A state feedback of the form $\mathbf{v} = -K\tilde{\mathbf{x}}^2$ can stabilize (6), where K can be obtained, e.g., by LQR design. Choose, for instance, $R = I_4$ and $Q = diag(10, 1, 10, 1)$ (these values are used in our simulation in Section 2.1). Provided $\gamma(x_1) \neq 0$, the closed-loop linear subsystem is exponentially stable and u_1 and u_2 are bounded.

By applying the transformation

$$\begin{aligned} z_1 &= \tilde{x}_1 \\ z_2 &= \tilde{x}_1 + \tilde{x}_2. \end{aligned} \tag{7}$$

to subsystem (4), we get

$$\begin{aligned} \dot{z}_1 &= z_2 - z_1 \\ \dot{z}_2 &= -\tilde{\epsilon}z_2[(z_2 - z_1)^2 + (z_1)^2]. \end{aligned} \tag{8}$$

Consider now the Lyapunov function candidate $V(\mathbf{z}) = \frac{1}{2}z_1^2 + \frac{1}{2}z_2^2$ whose derivative is given by

$$\begin{aligned} \dot{V}(\mathbf{z}) &= -z_1^2 + z_1z_2 - \tilde{\epsilon}z_2^2[z_1^2 + (z_2 - z_1)^2] \\ &\leq -\frac{z_1^2}{2} - \left\{\tilde{\epsilon}\left[z_1^2 + (z_2 - z_1)^2\right] - \frac{1}{2}\right\}z_2^2. \end{aligned} \tag{9}$$

$\dot{V}(\mathbf{z})$ is negative definite outside the ellipsoid $\Omega = \left\{\mathbf{z} \in \mathbb{R}^2 | z_1^2 + (z_2 - z_1)^2 \leq \frac{1}{2\tilde{\epsilon}}\right\}$ and, therefore, V decreases in Ω.

Let $\mathcal{V}_d = \{\mathbf{z} \in \mathbb{R}^2 | V(\mathbf{z}) \leq d\}$ and notice that $d = \frac{1}{\sqrt{2\tilde{\epsilon}}}$ is the smallest real number guaranteeing that $\Omega \subset \mathcal{V}_d$. From this observation, and since $\dot{V} < 0$ outside of $\mathcal{V}_d$, $\dot{V} < 0 \quad \forall V > \frac{1}{\sqrt{2\tilde{\epsilon}}}$; hence, $\mathcal{V}_d$ is positively invariant for all $d > \frac{1}{\sqrt{2\tilde{\epsilon}}}$.

Consider now the function $V_E(\mathbf{z}) = \frac{z_2^2}{2}$, then

$$\dot{V}_E(\mathbf{z}) = -\tilde{\epsilon}z_2^2[(z_2 - z_1')^2 + z_1^2] \leq 0, \forall \mathbf{z} \in \mathbb{R}^2 \tag{10}$$

Let $E = \{\mathbf{z} \in \mathcal{V}_d | \dot{V}_E(\mathbf{z}) = 0\} = \{\mathbf{z} \in \mathcal{V}_d | z_2 = 0\}$. For any trajectory in E, the dynamics of (8) are given by

$$\begin{aligned} \dot{z}_1 &= -z_1 \\ \dot{z}_2 &= 0 \end{aligned} \tag{11}$$

(11) proves E invariant; therefore, by LaSalle theorem, every solution starting in $\mathcal{V}_d$ approaches E as $t \to \infty$. Moreover, from (11), $z_1 \to 0$ on E. Since $\mathcal{V}_d$ is compact, all trajectories are bounded and it follows that, for all $\mathbf{z}(0) \in \mathcal{V}_d$, $\mathbf{z}(t) \to 0$. Again, this holds for all d such that $d > \frac{1}{\sqrt{2\tilde{\epsilon}}}$.

The determination of an estimate of the DOA of the origin $\tilde{\mathbf{x}} = 0$ requires the computation of the

set where the control input is well defined: $\mathcal{D} = \{\tilde{\mathbf{x}} \in \mathbb{R}^6 | u_4 \in \mathbb{R}, \phi(x_1) \neq 0, \gamma(x_1) \neq 0\}$. From (3)

$$\mathcal{D} = \{\tilde{\mathbf{x}} \in \mathbb{R}^6 \mid 0 \leq R'(\tilde{\mathbf{x}}), \phi(x_1) \neq 0, \gamma(x_1) \neq 0\} \quad (12)$$

where

$$R'(\tilde{\mathbf{x}}) = \psi^2(\tilde{x}_1 + x_1^d) + 4\phi(\tilde{x}_1 + x_1^d)R(\tilde{\mathbf{x}}). \quad (13)$$

Since (12) includes the full state, it describes a set that is hard to visualize. It is possible, however, to obtain a simple, although conservative, inner approximation of such set by bounding $\mathbf{v}(\tilde{\mathbf{x}}^2)$, which implies bounding $\tilde{\mathbf{x}}^2(0)$.

More specifically, let $\phi(t, \tilde{\mathbf{x}}_0^2)$, with $\tilde{\mathbf{x}}_0^2 = \tilde{\mathbf{x}}^2(0)$, be the solution of the closed-loop linear system (5) under the action of linear state feedback. Then, we have that

$$\mathbf{v}(\tilde{\mathbf{x}}^2) = -K\phi(t, \tilde{\mathbf{x}}_0^2). \quad (14)$$

Let $\{e_1, \dots e_4\}$ denote the natural basis in $\mathbb{R}^4$, and let $\phi_j(t) = \phi(t, e_j)$ be the response of the system subject to the initial condition e_j. Since the closed-loop linear system is stable, all solutions $\phi_j(t)$ are bounded. Let $\tilde{x}_j(0)$ be the entries of $\tilde{\mathbf{x}}_0^2$. Because of linearity, we have that

$$\tilde{\mathbf{x}}^2(t) = \sum_{j=1}^{4} \tilde{x}_j(0)\phi_j(t), \quad (15)$$

and hence

$$\mathbf{v}(\tilde{\mathbf{x}}^2(t)) = -K\sum_{j=1}^{4} \tilde{x}_j(0)\phi_j(t). \quad (16)$$

By denoting $K = [K_1^T \; K_2^T]^T$, it follows that

$$\|v_i(\tilde{\mathbf{x}}^2(t))\|_2 = \left\|K_i[\phi_1(t), \dots, \phi_4(t)]\tilde{\mathbf{x}}_0^2\right\|_2, i = 1, 2 \quad (17)$$

Since $v_i(\tilde{\mathbf{x}})$ enter into (12) squared, it is sufficient to find upper bounds to their 2-norms:

$$\sup_t \|v_j(\tilde{\mathbf{x}})\|_2 = \sup_t \left\|K_i[\phi_1(t), \dots, \phi_4(t)]\tilde{\mathbf{x}}_0^2\right\|_2 \quad (18)$$

$$\leq \left\|K_i[\sup_t |\phi_1(t)|, \dots, \sup_t |\phi_4(t)|]\tilde{\mathbf{x}}_0^2\right\|_2. \quad (19)$$

Then, an upper bound to $\|v_j(\tilde{\mathbf{x}}^2(t))\|_2$ is given by

$$\|v_j(\tilde{\mathbf{x}}^2(t))\|_2 \leq \left\|K_i[\lambda_1, \dots, \lambda_4]\tilde{\mathbf{x}}_0^2\right\|_2 \triangleq \bar{v}_i \quad (20)$$

where the values $\lambda_j = \sup_t |\phi_j(t)|$ are computed numerically by constraining the initial condition $\tilde{\mathbf{x}}_0^2$ inside a set $\mathcal{W} = \{\tilde{\mathbf{x}}_0^2 \in \mathbb{R}^4 | |\tilde{x}_i| \leq \omega_i, i = 3, \dots, 6\}$, for predefined values of ω_i. Choice of $\omega_3 = 0.1, \omega_4 = 1, \omega_5 = 0.1, \omega_6 = 1$ yields $\bar{v}_1 = \bar{v}_2 = 3.0226$.

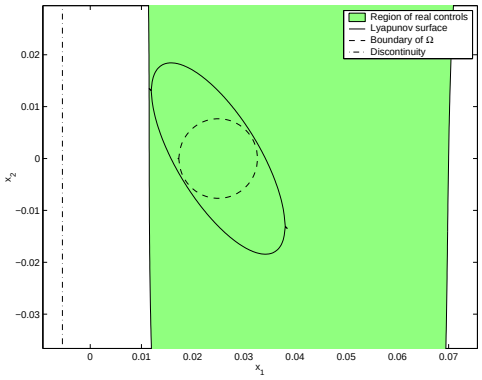

Figure 2: Estimate of the DOA for $x_1^d = 0.025$m

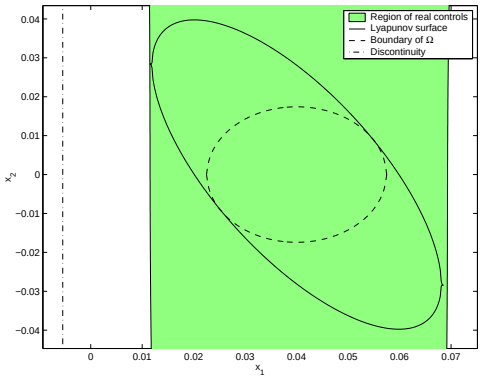

Figure 3: Estimate of the DOA for $x_1^d = 0.04$m

Then, $U(\tilde{\mathbf{x}})$, defined in (3), satisfies

$$U(\tilde{\mathbf{x}}) \leq \bar{U}(\tilde{\mathbf{x}}^1) \triangleq 2\left(\frac{\bar{v}_2}{2\gamma(\tilde{x}_1 + x_1^d)}\right)^2 + \left(\frac{\bar{v}_1}{\gamma(\tilde{x}_1 + x_1^d)}\right)^2 \quad (21)$$

Since $\phi(x_1) \geq 0$ in the range of interest, it follows that

$$\begin{aligned} R(\tilde{\mathbf{x}}) \geq \bar{R}(\tilde{\mathbf{x}}^1) \triangleq & \tilde{\epsilon}\,(\tilde{x}_1 + \tilde{x}_2)\,[\tilde{x}_1^2 + \tilde{x}_2^2] + \tilde{x}_2 \\ & - \phi(x_1)\bar{U}(\tilde{\mathbf{x}}^1) + G - \tilde{\chi}(x_1) \end{aligned} \quad (22)$$

which implies that

$$R'(\tilde{\mathbf{x}}) \geq \bar{R}'(\tilde{\mathbf{x}}^1) \triangleq \psi^2(\tilde{x}_1 + x_1^d) + 4\phi(\tilde{x}_1 + x_1^d)\bar{R}(\tilde{\mathbf{x}}^1). \quad (23)$$

Hence, the set

$$\hat{\mathcal{D}} = \{\tilde{\mathbf{x}}^1 \in \mathbb{R}^2 \mid 0 \leq \bar{R}'(\tilde{\mathbf{x}}^1), \phi(x_1) \neq 0, \gamma(x_1) \neq 0\} \quad (24)$$

is an inner approximation of the projection of $\mathcal{D}$ onto the $\tilde{\mathbf{x}}^1$ coordinates. Moreover, since the set can now be easily plotted, it can be verified that on $\{\tilde{\mathbf{x}}^1 \in \mathbb{R}^2 \mid 0 \leq \bar{R}'(\tilde{\mathbf{x}}^1)\}$, $\phi(x_1) \neq 0$,$\gamma(x_1) \neq 0$, and hence

$$\hat{\mathcal{D}} = \{\tilde{\mathbf{x}}^1 \in \mathbb{R}^2 \mid 0 \leq \bar{R}'(\tilde{\mathbf{x}}^1)\} \quad (25)$$

In conclusion, for given $\mathbf{x}_1^d$ and $\tilde{\epsilon}$, the largest value of d such that $\mathcal{V}_d \subset \hat{\mathcal{D}}$ determines an estimate of the DOA of

the origin of (4). Furthermore, given $\mathbf{x}(0) \in \mathcal{V}_d \times \mathcal{W} \subset \mathcal{D}$, the trajectories $\tilde{\mathbf{x}}^1(t)$ are bounded inside $\mathcal{V}_d$. Since E is attractive and $E \subset \mathcal{V}_d$, which is positively invariant, the trajectories $\tilde{\mathbf{x}}(t) \to E$ as $t \to \infty$. Furthermore, inside E, $\tilde{\mathbf{x}}(t) \to 0$ as $t \to \infty$. Since (5) is exponentially stable, the origin of the closed-loop system given by (4) and (5) is attractive for any initial condition lying inside $\mathcal{V}_d \times \mathcal{W}$, as stated on Theorem 1. □

In Figures 2 and 3, the shaded areas are parts of the set $\hat{\mathcal{D}}$, the solid ellipses represent the Lyapunov level surfaces $V = d$ for $d = 8.5 \times 10^{-5}$ and $d = 3.95 \times 10^{-4}$ respectively, while the dashed ellipses represent the Ω sets given by $\tilde{\epsilon} = 8,500$ and $\tilde{\epsilon} = 1,650$ respectively.

Remark: Note that the result of Theorem 1 guarantees boundness of $\mathbf{x}$ and attractiveness of the equilibrium $\mathbf{x}^d$, but not Lyapunov stability.

2.1 Simulation Results

Figures 4 and 5 show the state response and Figure 6 shows the control inputs of the closed-loop system when $\mathbf{x}_0 = [0.047, 0, -0.05, 0, 0.05, 0]^T$, $\mathbf{x}^d = [0.055, 0, 0, 0, 0, 0]^T$, and $\tilde{\epsilon} = 1,650$.

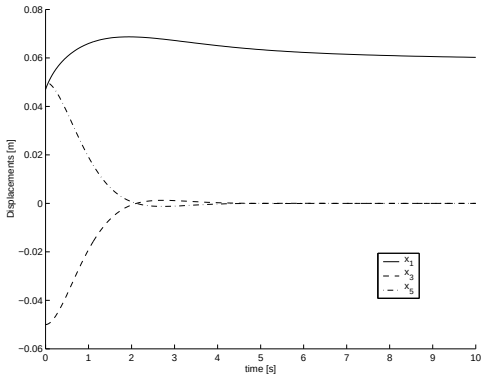

Figure 4: Transient position under Lyapunov control

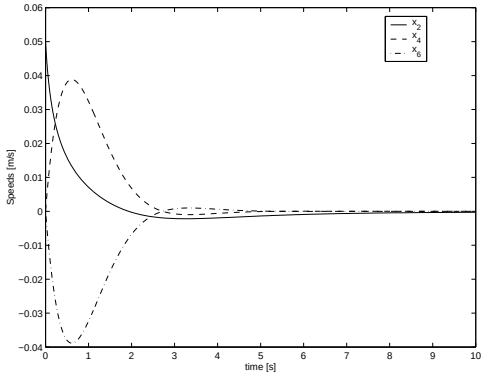

Figure 5: Transient speed under Lyapunov control

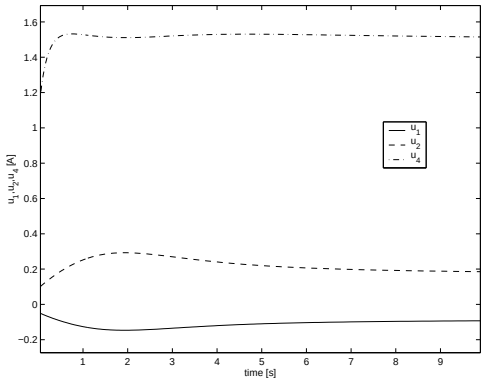

Figure 6: Control inputs u_1,u_2, and u_4 under Lyapunov control

3 Invariance control design

Consider again the controller (3), but consider a new control input u_4 replacing $R(\tilde{\mathbf{x}}^1)$ in (3) by

$$R(\tilde{\mathbf{x}}^1) = -u - \phi(x_1)U + G - \tilde{\chi}(x_1). \tag{26}$$

The new controller fully linearizes system (1) so that the $\tilde{\mathbf{x}}^1$ dynamics become

$$\tilde{\mathbf{x}}^1 \quad : \quad \begin{cases} \dot{\tilde{x}}_1 = \tilde{x}_2 \\ \dot{\tilde{x}}_2 = u. \end{cases} \tag{27}$$

Control law (26), together with proper stabilizing feedback $u = -K\tilde{\mathbf{x}}^1$, guarantees exponential stability of (4), provided that the value of u_4 exists. Accordingly, invariance of an estimate $\mathcal{N}$ of the set $\mathcal{M} = \left\{\mathbf{x} \in \mathbb{R}^6 | u_4 \in \mathbb{R}\right\}$ is pursued. In order to enlarge $\mathcal{N}$, we employ the method presented in [2] with some modifications in order to handle the fact that the size of $\mathcal{M}$ is directly affected by the control in the transformed input domain, u. Specifically, rather than (26), consider the dynamic feedback

$$R(\tilde{\mathbf{x}}^1) = -z - \phi(x_1)U + G - \tilde{\chi}(x_1) \tag{28}$$

$$\dot{z} = u, \tag{29}$$

so that the argument of the square root in (3) depends only on the state and not on the input. As a result, the $\tilde{\mathbf{x}}^1$ subsystem becomes

$$\tilde{\mathbf{x}}^1 \quad : \quad \begin{cases} \dot{\tilde{x}}_1 = \tilde{x}_2 \\ \dot{\tilde{x}}_2 = z \\ \dot{\tilde{z}} = u \end{cases} \tag{30}$$

From (29), $\mathcal{M} = \{\tilde{\mathbf{x}}^1 \in \mathbb{R}^2, z \in \mathbb{R} \,|\, \psi(\tilde{x}_1 + x_1^d)^2 + 4\phi(\tilde{x}_1 + x_1^d)\left[-z - \phi(\tilde{x}_1 + x_1^d)U + G - \tilde{\chi}(\tilde{x}_1 + x_1^d)\right] \geq 0\}$. Since $\mathcal{M}$ does not anymore depend on u, invariance control

can now be applied. First, define the transformation

$$\begin{bmatrix} \xi_1 \\ \xi_2 \\ y \end{bmatrix} = \begin{bmatrix} \tilde{x}_1 \\ \tilde{x}_2 \\ k_1\tilde{x}_1 + k_2\tilde{x}_2 + k_3 z \end{bmatrix} \tag{31}$$

and the passifying feedback

$$u = \frac{1}{k_3}\left(v - (2Q_{12}^T P_{11} - Q_{21})[\xi_1, \xi_2]^T - Q_{22} y\right) \tag{32}$$

where v is an external input, k_1, k_2, k_3, $Q_{11}, Q_{12}, Q_{21}, Q_{22}, P_{11}$ are as defined in [2] with

$$T = \begin{bmatrix} 1 & 0 & 0 \\ 0 & 1 & 0 \end{bmatrix} \qquad W_{11} = I_2.$$

The transformation (31) and the feedback (32) map (30) to

$$\begin{aligned} \dot{\xi} &= \begin{bmatrix} 0 & 1 \\ -\frac{k_1}{k_3} & -\frac{k_2}{k_3} \end{bmatrix} \xi + \begin{bmatrix} 0 \\ \frac{1}{k_3} \end{bmatrix} y \\ \dot{y} &= -2Q_{12}^T P_{11}[\xi_1, \xi_2]^T + v, \end{aligned}$$

which is exponentially stable for any feedback of the form $v = -\alpha(t)y$ for any switched constant $\alpha(t) > 0$.

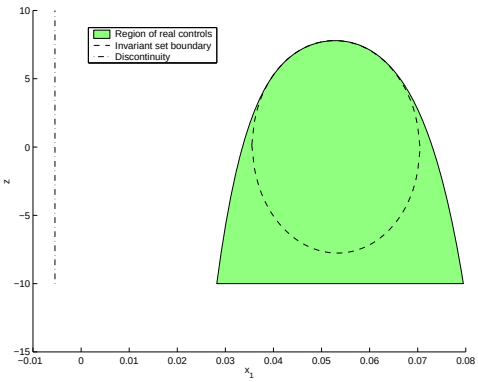

Figure 7: Projection of $\mathcal{M}$ and $\mathcal{N}$ on the (x_1, z) plane

In order to apply the methodology in [2], we need to approximate $\mathcal{M}$ by a set $\mathcal{N} \subset \mathcal{M}$ with desired properties. Let $\Phi : \mathbb{R}^3 \to \mathbb{R}$ be a C^1 function such that $\mathcal{N} = \{(\xi_1, \xi_2, y) | \Phi(\xi_1, \xi_2, y) \leq 0\}$. For a large $\mathcal{N}$, choose

$$\begin{aligned} \Phi(\xi_1, \xi_2, y) =& a(\xi_1 + x_1^d - x_1')^2 + b\xi_2^2 - r^2 \\ &+ c(x_1' - \xi_1 - x_1^d)\xi_2 + dy^2 \end{aligned} \tag{33}$$

which describes a 3D ellipsoid centered at $(x_1', 0, 0)$. The positive constants a, b, c, d and x_1' determine the shape and size of the set $\mathcal{N}$. Figure 7 shows both $\mathcal{M}$ and $\mathcal{N}$ in original x_1, z coordinates for a given set of parameters. Positive invariance of $\mathcal{N}$ requires $\dot{\Phi}(\xi_1, \xi_2, y) < -\epsilon < 0, \epsilon \in \mathbb{R}^+$ at $\partial\mathcal{N}$, the boundary of $\mathcal{N}$. Differentiation of Φ and Young inequality yield

$$\begin{aligned} \dot{\Phi} \leq& \left\{a + \frac{c}{2k_3}(k_2 + k_1)\right\}(\xi_1 - x_1' + x_1^d)^2 \\ &+ \left\{a - c + \frac{ck_2}{2k_3} + \frac{b}{k_3}(k_1 - 2k_2)\right\}\xi_2^2 \\ &+ \frac{k_1}{k_3}\left(b + \frac{c}{2}\right)\xi_1^2 + F(y) \end{aligned} \tag{34}$$

where $F(0) = 0$. Then, k_1, k_2, and k_3 determine whether $\dot{\Phi}(\xi_1, \xi_2, y = 0) < 0$, yielding a set of linear inequalities whose solution can be found through the linear programming problem

$$\begin{array}{c} \min \quad C^T k \\ A_{op} k \leq b_{op} \\ k > 0 \end{array} \tag{35}$$

where $C = [c_1,\ c_2,\ c_3]$ is a vector of design parameters, $b_{op} = -[\kappa,\ \kappa]^T$, $\kappa \in \mathbb{R}^+$ and

$$A_{op} = \begin{bmatrix} c & c & 2a \\ 2b & c - 4b & 2a - 2c \end{bmatrix}. \tag{36}$$

Because the weighting vector C introduces extra degrees of freedom, solving the set of inequalities as an LP problem conveys two advantages. First, it allow us to individually affect the speeds of convergence of $\tilde{x}_1, \tilde{x}_2$ and z. Second, the geometric characteristics of the zero dynamics plane $(y = 0)$ can be freely set.

Following [2], switching of α every time that the trajectory hits $\partial\mathcal{N}$ guarantees asymptotic stability for $y \neq 0$. In addition, α must be positive in order to maintain stability of the closed loop system. A choice of α that satisfies both requirements at the $j-$th switching is

$$\alpha_j = \frac{\epsilon + \frac{\partial\Phi}{\xi_1}\dot{\xi}_1 + \frac{\partial\Phi}{\xi_2}\dot{\xi}_2 - 4dyQ_{12}^T P_{11}[\xi_1, \xi_2]^T}{2dy^2} \tag{37}$$

3.1 Simulation Results

The simulation of the invariance controller used the set of values: $r = 0.12$, $a = 80$, $b = 0.5$, $c = -5$, $d = 2$, $x_1' = 0.048$, $C = [0.1, 1, 1]^T$, $\kappa = 1$, $\mu = 0.001$, $\alpha(0) = 1$ and $\epsilon = 1\times10^{-6}$. The LP algorithm generated $k = [0.1175, 0.4025, 0.01]^T$.

Figures 8 and 9 show the x_1 and x_2 response for $\mathbf{x}_0 = [0.047, 0.05, -0.05, 0, 0.05, 0]^T$, $z(0) = 0$ and $x^d = [0.055, 0, 0, 0, 0, 0]$. Figure 10 presents the respective control inputs u_1,u_2, and u_4. Figure 11 shows the evolution of the trajectory (the bold curve) making noticeable that it remains inside the set $\mathcal{N}$, whose boundary is given by the 3D ellipsoid also depicted there. For this simulation, two switchings occurred.

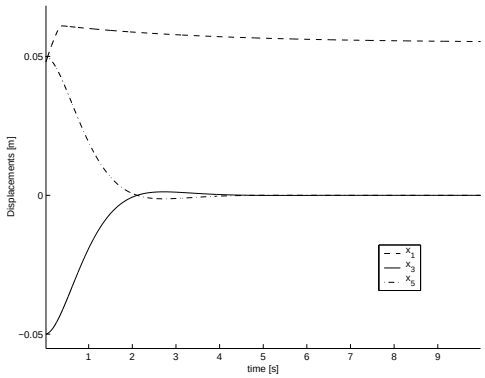

Figure 8: Transient position under invariance control

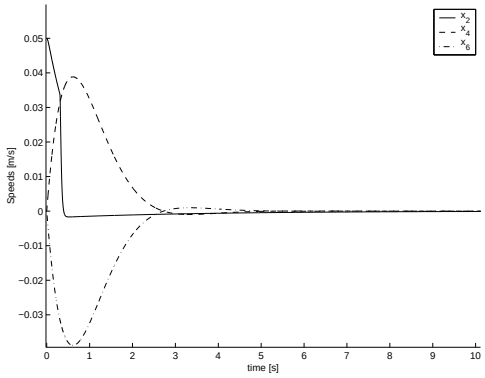

Figure 9: Transient speed under invariance control

4 Controllers' comparison

The first controller has steady state currents of up to 1.3A and, in the best case, the DOA is limited inside $0.02 < x_1 < 0.06$. Its speed of response significantly varies with the initial conditions. On the other hand, the invariance controller also requires currents as large as 1.3A for steady state and 1.5A for transient. The corresponding DOA lies inside $0.035 < x_1 < 0.07$. The speed of convergence also depends on the initial conditions but it is faster when switching does not occur. Therefore, when compared to the first nonlinear controller, the invariance-based one achieves the fastest response but also higher control effort.

5 Conclusions

We have introduced and analyzed two nonlinear controllers achieving set-point stabilization for a three degrees-of-freedom magnetic levitation system. Because, under non-ideal conditions, the device does not prevent rotation of the platen, an apparatus with 5 controlled DOF will replace this design. Future work will also design robust adaptive controllers taking into account disturbances and model uncertainties. An experimental setup is being built to test the designed controllers.

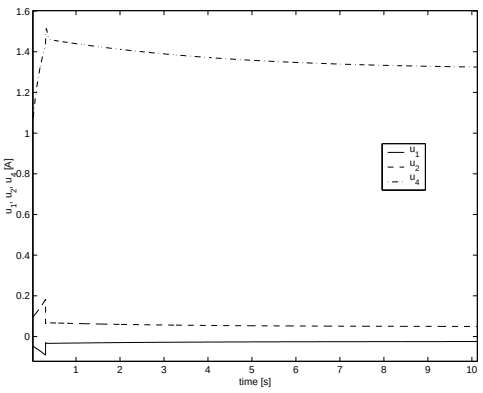

Figure 10: Control inputs u_1,u_2, and u_4 under invariance control

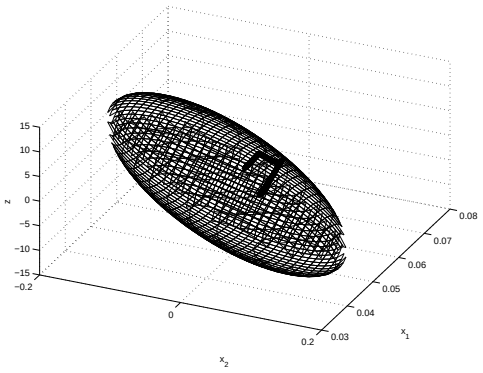

Figure 11: System's trajectory under invariance control

References

[1] W. Kim and D.L. Trumper, "High-precision levitation stage for photolithography", in *Precision Engineering* vol. 22, pp. 66-77, 1998

[2] J. Mareczek, M. Buss and M.W. Spong "Invariance Control for a Class of Cascade Nonlinear Systems", in *IEEE Transactions on Automatic Control* vol. 47, no. 4, pp. 636-640, 2002

[3] R. Becerril-Arreola and M. Maggiore, "Modeling for control of a three degrees-of-freedom Magnetic Levitation System", SCG Technical Report, Univ. of Toronto, 2002, `http://www.control.utoronto.ca/tech_reports/tech_reports.html`